2023 IEEE 26th International Conference on
Intelligent Transportation Systems (ITSC)
24-28 September 2023. Bilbao, Bizkaia, Spain

Intelligent Adaptive Electric Vehicle Motion Control for Dynamic Wireless Charging

Lokesh Chandra Das[1], Dipankar Dasgupta[1], and Myounggyu Won[1]

2023 IEEE 26th International Conference on Intelligent Transportation Systems (ITSC) | 979-8-3503-9946-2/23/$31.00 ©2023 IEEE | DOI: 10.1109/ITSC57777.2023.10422064

***Abstract*— Dynamic wireless charging (DWC) is an emerging technology designed to enable electric vehicles (EVs) to be wirelessly charged while in motion. It is gaining significant momentum as it can potentially address the limited range problem for EVs. However, due to the significant power loss caused by wireless power transfer, improving the charging efficiency remains as a major challenge. This paper presents the first Long Short-Term Memory (LSTM)-based EV motion control system for DWC with an aim to maximize the charging efficiency. The dynamics of the electromagnetic field generated from the transmitter coils of a DWC system are effectively captured using a machine-learning approach based on the multi-layer LSTM. The multi-layer LSTM model is used to predict the location where the electromagnetic strength is expected to be maximal and to control the lateral position of EV accordingly to optimize the charging efficiency. Extensive simulations were conducted to demonstrate that our LSTM-based EV motion control system achieves by up to 174% higher charging efficiency compared with existing vehicle motion control systems focused on keeping an EV in the center of the lane.**

I. Introduction

Energy security is one of the highest priorities for many countries. The largest energy consumer is the transportation industry [1]. For instance, in U.S., the transportation industry alone consumed more than 28% of the total energy in just one year [1]. Especially, gasoline fuel consumption mostly for vehicles accounts for more than 56% of the total transportation energy consumption [1]. Electric vehicles (EVs) have received significant attention as a viable solution to reduce energy consumption and alleviate environmental effects. However, developing inexpensive, durable, and reliable energy storage system remains as a major challenge. In fact, one of the primary concerns that discourage purchase of an EV for many consumers is the range anxiety and the long battery charging time [2].

Along with numerous automation technologies for Intelligent Transportation Systems [3]–[5], dynamic wireless charging (DWC) is an emerging technology designed to address the limited range issue [6], [7]. The DWC technology allows EVs to be wirelessly charged while in motion based on the magnetic coupling between the transmitter coils embedded under the road surface and the receiver coils fit in an EV [8]. More specifically, the transmitter coils are provided with a high-frequency current and generate electromagnetic field, which is picked up by the receiver coils of the EV to charge the battery [7]. The first concept of DWC was designed by Bolger *et al.* [9] in 1978. Since then, extensive research has been conducted to develop numerous DWC solutions [2], [7], [10].

To achieve broader acceptance of DWC systems as a convenient, reliable, and flexible solution for charging EVs, there are some challenges to be addressed [2]. One of the most significant hurdles is the reduced power transfer efficiency caused by the physical misalignment between the transmitter and receiver coils [11]–[15]. Since EVs are charged while in motion, temporary misalignment is inevitable, which causes significant fluctuation of power transfer efficiency [16].

Numerous works have been proposed to mitigate the impact of misalignment. Hardware-based solutions are focused on modifying [17], [18] or adding [19], [20] a new hardware component, *e.g.,* changing the geometry or configuration of the coil to improve the power transfer efficiency. Tracking-based approaches are designed to align the EV in the center of the lane by utilizing a vehicle positioning algorithm [15], [21]. Vision-based solutions track the lateral position of EV using the cameras to position the EV in the center of the lane [16]. However, a limitation of these solutions is that the dynamics of the electromagnetic field generated from the transmitter coils of the DWC system are not taken into account to control the EV motion, thereby potentially leading to degraded power transfer efficiency [22].

In this paper, we present an LSTM-based adaptive EV motion control system for DWC. To optimize the power transfer efficiency, the lateral position of an EV is adaptively adjusted in response to the dynamics of the electromagnetic field generated by the transmitter coils of a DWC system. We design a multi-layer LSTM network that effectively captures the dynamics of the electromagnetic field. The LSTM model allows the EV to predict the lateral position where the power transfer efficiency is expected to be maximized and control its motion to align with the optimal position. Through extensive simulations, we uncover, for the first time, the strong potential of the machine learning-driven approach for DWC effectively modeling the dynamics of the electromagnetic field of the transmitter coils to significantly boost the power transfer efficiency. More specifically, compared with a state-of-the-art approach focused on keeping the EV in the center of the lane to improve the power transfer efficiency, we demonstrate that our LSTM-based approach leveraging the prediction of the optimal lateral position where the electromagnetic strength is maximized enhances the power transfer efficiency by up to 174%.

This paper is organized as follows. In Section II, we thoroughly review solutions designed to address the misalignment problem for DWC. We then perform a motivational study to

[1]Department of Computer Science, University of Memphis, TN, 38152, USA {ldas,ddasgupt,mwon}@memphis.edu

Authorized licensed use limited to: WICHITA STATE UNIVERSITY LIBRARIES. Downloaded on September 09,2025 at 19:54:10 UTC from IEEE Xplore. Restrictions apply.

better understand the dynamics of the electromagnetic field generated by the transmitter coils in Section III. And then, we present the details of the design of the proposed LSTM model in Section IV. The simulation results are presented in Section V followed by conclusion and future work in Section VI.

II. Related Work

This section reviews the literature on the misalignment problem for DWC. We categorize various latest works into hardware-based, tracking-based, and vision-based approaches.

The hardware-based approaches are characterized by modifying the hardware of the DWC system to address the misalignment problem. Chen *et al.* propose a novel geometry of coils to improve power transfer efficiency [17]. Chow *et al.* consider placing multiple coils in an orthogonal configuration [18]. Kalwar *et al.* combine multiple coils of different geometry into a single unit [23]. Some hardware-based approaches attempt to add a new hardware component. For instance, E-shape or U-shape ferrite cores are integrated with the source coils [19], [20]. Active coil resonance frequency tuning circuits are applied [24], [25]. A novel arrangement method for sensing coils is developed to detect lateral misalignment problem [26]. Although these hardware-based approaches improve the power transfer efficiency, the dynamics of the electromagnetic field are not considered. Additionally, some approaches have limitations in terms of the space and weight constraints for specific environments [15].

The tracking-based approaches are focused on monitoring the alignment between the EV and the transmitter coils using a vehicle position tracking system. Global positioning system (GPS) has been widely adopted for tracking the EV position. However, due to the high positioning error of GPS, most tracking-based approaches utilize different types of sensors for tracking the EV position. For instance, a radio-frequency identification (RFID) tag or a magnetic marker has been adopted [27]–[29]. However, since the strength of the magnetic field decays rapidly as the distance between the detector and the marker increases, those magnetic markers or RFID tags must be placed very close to each other to achieve high-resolution tracking performance, thereby increasing the construction cost significantly. In an effort to address this problem, sensor systems with greater range have been integrated with the charging system [30]. Additionally, a Gaussian function-based algorithm is developed to increase the detection accuracy [21]. However, these tracking system-based approaches do not work effectively when the vehicle speed is very high since the magnetic field changes dynamically as the vehicle moves at a fast speed [15].

The inherent limitations of the tracking-based approaches have been addressed by developing the autonomous coil alignment system (ACAS) [31]. The main advantage is that it is designed to track the vehicle's misalignment position based only on the voltage changes in the vehicle's load coil [31]. An enhanced version of ACAS has been introduced to reduce the complexity of the algorithm and hardware [15], allowing for wider applicability for DWC systems with varying specifications. ACAS not only addresses the challenges of external sensor-based approaches since it is implemented on top of the existing DWC system but also reduces the implementation cost. Although ACAS is demonstrated as an effective solution for addressing the misalignment problem, it is only compatible with specific DWC systems. Furthermore, ACAS does not account for the effect of the dynamically changing electromagnetic field of the transmitter coils on the power transfer efficiency [15].

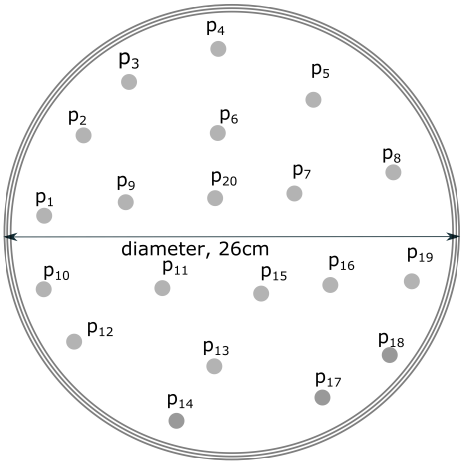

Fig. 1. The transmitter coil and 20 random points where the electromagnetic strength is measured. Varying electromagnetic strength is measured at each point when an EV equipped with the receiver coil passes over the transmitter coil.

The vision-based approaches have been proposed recently that rely on the cameras of the EV to track the lateral position of the EV to keep the vehicle in the center of the lane to improve the power transfer efficiency [16]. However, due to the dynamically changing electromagnetic field, positioning the EV in the center of the lane does not guarantee optimal power transfer efficiency. In contrast to existing works, our solution is the first machine learning-driven approach that adaptively controls the EV position based on the prediction of the optimal position with maximum electromagnetic strength by effectively modeling the dynamics of the electromagnetic field.

III. Understanding the Dynamics of the Electromagnetic Field in DWC

We perform a simulation study to demonstrate the dynamics of the electromagnetic field generated from the transmitter coils of a DWC system. We use the QuickField software [32], an electromagnetic field simulation platform widely for various kinds of electromagnetic applications for electrical, thermal, bio-, and chemical engineering, to implement the realistic electromagnetic field generated from the non-linear coils of the DWC system under varying conditions.

A simulation environment is set up aiming to implement a general DWC system. The transmitter coils are installed under the ground, and the receiver coils are mobile mounted on the EV chassis. More specifically, the transmitter coils are at 3cm depth under the ground, and the shape of the coils (*i.e.*,

Authorized licensed use limited to: WICHITA STATE UNIVERSITY LIBRARIES. Downloaded on September 09,2025 at 19:54:10 UTC from IEEE Xplore. Restrictions apply.

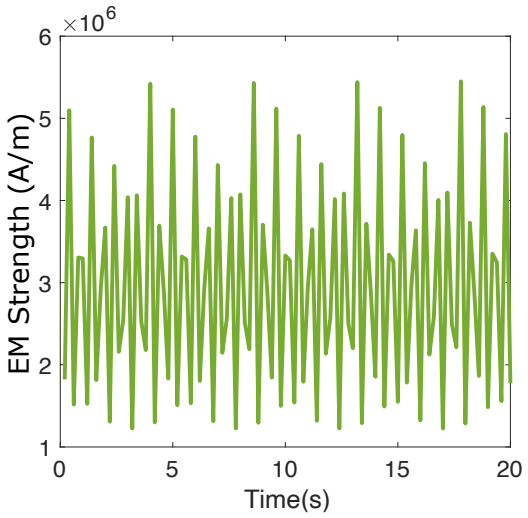

Fig. 2. Electromagnetic strength measured at a point over time. The result shows the strong temporal dynamics of the electromagnetic strength.

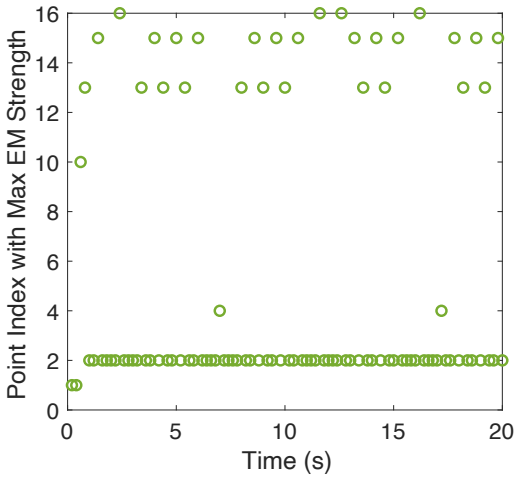

Fig. 3. Point indices with maximum electromagnetic strength. The result demonstrates the strong spatial dynamics of electromagnetic strength.

transmitter and receiver coils) is circular with a radius of 13 cm. As shown in Fig. 1, a total of 20 points are randomly and uniformly selected. We measure the electromagnetic strength at each point when the receiver coils pass over the transmitter coils. The electromagnetic strength is known to effectively represent the efficiency of wireless power transfer [33]–[35]. The measurement unit for the electromagnetic strength is A/m (*i.e.,* Ampere per meter). More precisely, the unit for magnetic permeability μ is defined as N/A^2 where N is Newton, and the magnetic field B is measured in Tesla which is N/Am. The magnetic field strength is then measured in $B/\mu = T/(N/A^2) = (N/Am)/(N/A^2) = A/m$.

We first demonstrate the time-varying characteristic of electromagnetic strength. Fig. 2 depicts the electromagnetic strength measured at a random point over a period of 20 seconds. As shown, the electromagnetic strength at this point changes dynamically over time. We repeat the same experiment at different points and observe similar temporal dynamics of the electromagnetic strength. We then evaluate the spatial dynamics of the electromagnetic field. In particular, we demonstrate that the maximum electromagnetic strength is not always observed at the center of the electromagnetic field. Fig. 3 depicts the indices of the points with the maximum electromagnetic strength measured at an interval of 1 second. The result shows that the point with the maximum electromagnetic strength also dynamically changes over time. The observed spatio-temporal dynamic of the electromagnetic strength around the transmitter coil presents a motivation to optimize the power transfer efficiency by predicting the optimal point with the maximum electromagnetic strength and aligning the EV with the optimal point before the EV reaches the point (without degrading the driver's comfort).

IV. LSTM-Based Adaptive Vehicle Motion Control for DWC

This section presents the details of the proposed LSTM-based adaptive vehicle motion control system for DWC. The goal is to model the dynamics of the electromagnetic field using LSTM to control the lateral position of the EV to optimize the power transfer efficiency. We start with an overview of the proposed system (Section IV-A), followed by the details of our dataset (Section IV-B). We then present the basics of LSTM in Section IV-C and the details of our LSTM model in Section IV-D.

A. System Overview

An overview of a DWC system integrated with our LSTM-based vehicle motion control solution is presented. The proposed DWC system consists of four main components: a power transfer module, a power receiver module, an EV motion controller, and a roadside unit (RSU). The contribution of this paper is focused on designing the EV motion controller. Fig. 4 depicts the system architecture of the DWC system. The power transfer module is installed beneath the road surface. The power receiver module is mounted on the EV chassis. Electric power is provided to the EV's battery via magnetic coupling resonance between the transmitter and receiver coils. The RSU is responsible for collecting the electromagnetic field data to train the LSTM model. The EV motion controller sends its speed information to the RSU via vehicle-to-everything (V2X) communication. The RSU then estimates the arrival time of the EV, based on which the RSU computes the EV's optimal lateral position using the LSTM model. The RSU then sends the optimal lateral position to the EV motion controller via V2X. The EV motion controller adjusts the vehicle motion to align the vehicle with the optimal lateral position to maximize the power transfer efficiency.

B. Dataset Preparation

In this section, a dataset used to train and test our LSTM model is explained. The same simulation setting described in Section III is used to collect the dataset. Specifically, we measure the electromagnetic strength at 20 points every 200ms. A point that has the largest electromagnetic strength

Authorized licensed use limited to: WICHITA STATE UNIVERSITY LIBRARIES. Downloaded on September 09,2025 at 19:54:10 UTC from IEEE Xplore. Restrictions apply.

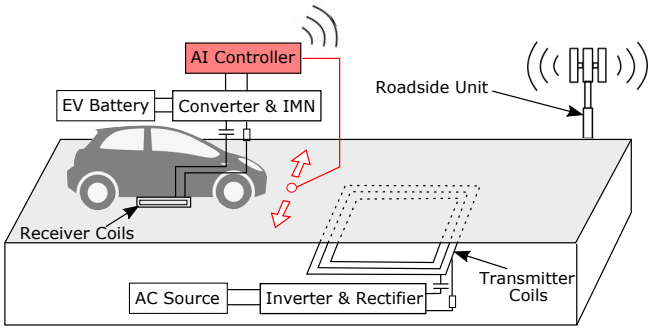

Fig. 4. An architecture of the dynamic wireless charging system integrated with the proposed LSTM-based vehicle position control system. The EV motion controller (EV) obtains the time-series electromagnetic data from the RSU and predicts the optimal lateral position of the EV using the data before it reaches the target transmitter coils to optimize the power transfer efficiency.

$$D_{Features} = \begin{bmatrix} \vec{x}_1 & \vec{x}_2 & \vec{x}_3 & \cdots & \vec{x}_{10} \\ \vec{x}_2 & \vec{x}_3 & \vec{x}_4 & \cdots & \vec{x}_{11} \\ \vec{x}_3 & \vec{x}_4 & \vec{x}_5 & \cdots & \vec{x}_{12} \\ \vdots & \vdots & \vdots & & \vdots \\ \vec{x}_{N-10} & \vec{x}_{N-9} & \vec{x}_{N-8} & \cdots & \vec{x}_{N-1} \end{bmatrix} \quad D_{Labels} = \begin{bmatrix} \vec{x}_{11} \\ \vec{x}_{12} \\ \vec{x}_{13} \\ \vdots \\ \vec{x}_N \end{bmatrix}$$

Fig. 5. An example of the preprocessed dataset. The dataset consists of features and labels prepared using the sliding window-based method for training and testing our LSTM model.

is recorded and used as a feature vector. More specifically, the feature vector $\overrightarrow{x_i}$ is denoted by $[T_i\ A_i\ p_x\ p_y]$ where T_i is the i-th time-step (the interval of time-step is 200ms), A_i is the electromagnetic strength, p_x and p_y are the coordinates of the point with the maximum electromagnetic strength. Consequently, our raw dataset consists of a sequence of feature vectors, $\{\overrightarrow{x_1},...,\overrightarrow{x_N}\}$.

The raw dataset, *i.e.,* a sequence of feature vectors is pre-processed to make it suitable for training and testing our LSTM model. We use the standard MinMaxScaler to scale up all feature values between 0 and 1 to allow our LSTM model to converge faster. A sliding window is applied to restructure the raw dataset. More specifically, a sliding window of size 10 comprising of 10 successive feature vectors is used to predict the point with the largest electromagnetic strength in the next time-step. The sliding window moves forward by one position. Fig. 5 shows an example of the converted dataset consisting of a feature matrix $D_{Features}$ and the corresponding label matrix D_{Label}. The i^{th} row of $D_{Features}$ represents 10 consecutive feature vectors used to predict the point with the largest electromagnetic strength in the next time-step which is specified in the i^{th} row of D_{Label}.

C. LSTM

Long Short-Term Memory networks (LSTMs) proposed by [36] are designed to learn long-term dependencies and effectively deal with the vanishing gradient problem [37], [38]. LSTM is highly suitable for applications that make predictions based on time series data [39].

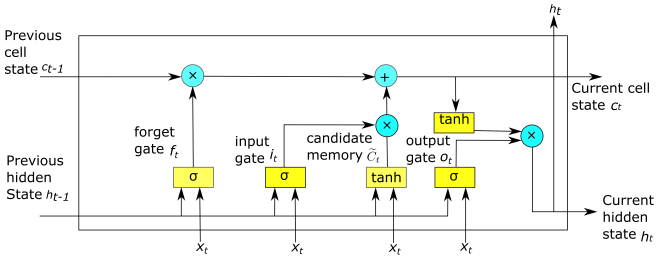

Fig. 6. A structure of an LSTM cell. The LSTM cell is a basic building block of the proposed multi-layer LSTML model.

A memory block is the basic unit of the LSTM architecture. Each memory block consists of one or more memory cells along with the input, output, and forget gates. Fig. 6 displays the internal structure and operations of an LSTM cell. The forget gate f_t controls which information is to be kept and which is to be discarded based on the current input x_t and the previous hidden state h_{t-1}, being passed through the sigmoid activation function σ. The input gate i_t decides which information is necessary for the current state and which is irrelevant based on the output of the sigmoid activation function with x_t and h_{t-1} as input. Eq. (1) displays the mathematical representations of f_t and i_t

$$f_t = \sigma(W_h^f h_{t-1} + W_i^f x_t + b_f),$$
$$i_t = \sigma(W_h^i h_{t-1} + W_i^i x_t + b_i), \quad (1)$$

where W_h^* and W_i^* are the weight matrices for the previous hidden state h_{t-1} and current input vector x_t of corresponding gates, respectively, and b_f and b_i are biases. An intermediate candidate value matrix $\widetilde{C}_t$ is computed based on the *tanh* activation function as shown in Eq. (2). Using the forget gate f_t, input gate i_t, and candidate value matrix $\widetilde{C}_t$, the old cell state c_{t-1} is updated with the new cell state c_t as displayed in Eq. (2).

$$\widetilde{C}_t = \tanh(W_h^c h_{t-1} + W_i^c x_t + b_c),\ c_t = f_t \otimes c_{t-1} + i_t \otimes \widetilde{C}_t, \quad (2)$$

where b_c is a bias, and $\otimes$ indicates element-wise multiplication. The output gate o_t regulates what to output to the next cell, *i.e.,* the value of the next hidden state h_t with operations shown in Eq. (3).

$$o_t = \sigma(W_h^o h_{t-1} + W_i^o x_t + b_o),\ h_t = \tanh(c_t) \otimes o_t, \quad (3)$$

where b_o is a bias.

D. LSTM Model Design

Adaptive EV position control to optimize the power transfer efficiency can be modeled as a multivariate time series prediction problem: at any time-step t, a future position with the maximum electromagnetic strength is inferred based on the past optimal positions. More specifically, our objective is to predict the future optimal points at time steps (T_{t+1}, $T_{t+2},...,T_{t+f}$), where t is the current time step, and f is the

Authorized licensed use limited to: WICHITA STATE UNIVERSITY LIBRARIES. Downloaded on September 09,2025 at 19:54:10 UTC from IEEE Xplore. Restrictions apply.

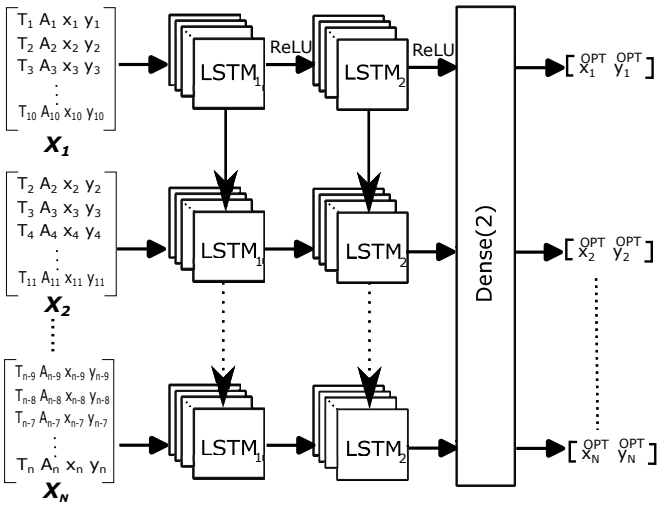

Fig. 7. The architecture of the multi-layer LSTM model. The model predicts the future optimal point based on 10 feature vectors at each time step.

future prediction horizon, based on the past optimal points that have the largest electromagnetic strengths at time steps (T_{t-l}, T_{t-l+1},...,T_t) where l is the length of past observations. In this paper, we set f to 1 and l to 10. Note that these parameters can be easily adapted to meet the needs of different application requirements.

To solve the problem, we design a multi-layer LSTM model using the basic LSTM network as a building block. Fig. 7 displays the architecture of the multi-layer LSTM model. As it can be seen, the input to train the LSTM model is a sequence of 10×4 matrices $\{X_1, ..., X_N\}$ where each matrix contains 10 successive feature vectors (*i.e., l* is set to 10 in our model). Essentially, an input matrix represents a single row of the feature matrix $D_{Features}$. More specifically, the 10 feature vectors of an input matrix at time-step t denoted by $\{\vec{x}^{(t-l+1)}, \vec{x}^{(t-l+2)}, ..., \vec{x}^{(t)}\}$ are fed into the first LSTM layer denoted by LSTM_1. The first LSTM layer outputs a sequence of feature vectors as an input for the following LSTM layer denoted by LSTM_2, which is directly connected to the dense layer that produces the coordinates of the point with the maximum electromagnetic strength at time-step $t+1$. Since predicting a 2D optimal position is a regression problem, the output of the fully connected layer is passed through the linear activation function. We train the model with the mean squared error (MSE) loss function representing the difference between the ground-truth optimal point and the predicted point: $MSE = \frac{1}{K}\sum_{i=1}^{K}(Y_i - \hat{Y}_i)^2$, where K is the number of the training sample, Y_i is the actual value, and $\hat{Y}_i$ is the predicted value.

V. Simulation Results

The performance of the proposed machine learning-driven EV motion control system for DWC is evaluated. We used the QuickField simulation software [32] to simulate the electromagnetic field generated from the transmitter coils of a DWC system. A 2D point with the maximum electromagnetic strength was recorded with a time-step interval of 200ms. Specifically, a feature vector $\overrightarrow{x_i} = [T_i\ A_i\ p_x\ p_y]$ was created at each time-step i by manually measuring electromagnetic strength at 20 points selected uniformly at random and finding the one with the maximum electromagnetic strength. To train our LSTM model, a total of 6,000 feature vectors corresponding to 20 minutes of DWC operation time were created, which took over 70 hours due to the tedious manual measurement process. In this section, we demonstrate that even with the relatively short operation time, the charging efficiency can be significantly improved.

A key metric used in this evaluation study to represent the charging efficiency is electromagnetic strength. In fact, electromagnetic strength is known to be directly related to charging efficiency and has been used to measure performance in much wireless charging systems [33]–[35]. More specifically, the charging efficiency is represented as the average of the electromagnetic strengths measured at the points that are aligned with the center of the EV's receiver coil during the course of the 20-minute operation time. The charging efficiency of the proposed approach was compared with existing solutions designed to enhance the charging efficiency by positioning the EV in the center of the lane [16]. We denote such a solution by the "Base" approach in our simulation study.

We start by determining the optimal hyperparameters for our LSTM model (Subsection V-A). Using the selected hyperparameters, we measure the charging efficiency by varying the dataset size and prediction frequency (Subsection V-B). We then conduct simulations to analyze the performance in terms of driver comfort (Subsection V-C) and effect of EV localization errors (Subsection V-D). Lastly, we measure the computational delay to analyze the real-world applicability of the proposed EV control system (Subsection V-E)

A. Hyperparameter Tuning

We carried out Hyperparameter tuning to determine the optimal parameters. The grid search method was used to find the optimal values for the number of hidden units, batch size, and learning rate for our LSTM model. For the grid search, we considered the number of hidden units between 40 and 180 with an interval of 20, a set of batch sizes $\{16, 32, 64, 128, 256\}$, and a set of learning rates $\{0.01, 0.001, 0.0001, 0.00001, 0.000001\}$. The mean squared error (MSE) between the actual (ground truth) coordinates and the model-predicted coordinates was used to represent the effectiveness of the selected hyperparameters. In our simulation setting, we found that the number of hidden units of 120, batch size of 16, and learning rate of 0.001 gave the best performance.

B. Charging Efficiency

In this section, we evaluate the charging efficiency of the proposed solution. The hyperparameters selected in Section V-A were used to train our LSTM model. The LSTM model was used to make 600 predictions to align the center of the receiver coil with the predicted points. The charging efficiency was measured by varying the size of our dataset and the prediction

Authorized licensed use limited to: WICHITA STATE UNIVERSITY LIBRARIES. Downloaded on September 09,2025 at 19:54:10 UTC from IEEE Xplore. Restrictions apply.

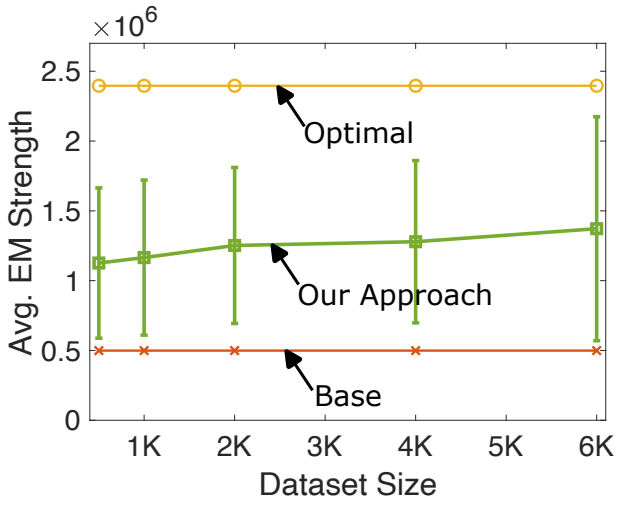

Fig. 8. Charging efficiency with varying size of the dataset. The result shows that the proposed solution improves the charging efficiency by 174% compared to that of the based method.

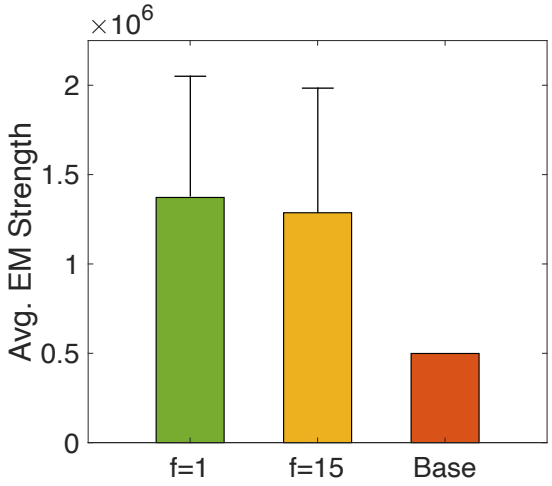

Fig. 10. A trade-off between charging efficiency and driver comfort. The value of 15 for parameter f represents the prediction frequency with minimal impact on driver comfort.

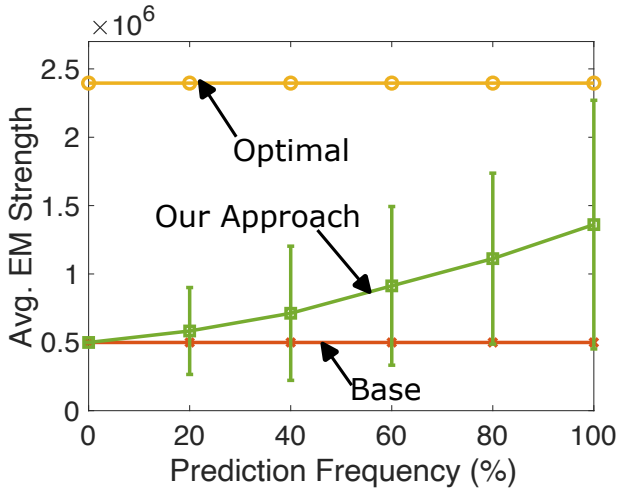

Fig. 9. Charging efficiency with varying prediction frequency. The charging efficiency of the proposed solution depends greatly on the prediction frequency.

frequency. In particular, the prediction frequency determines the rate at which the EV performs a prediction to control its lateral position. For example, a prediction frequency of 100% means that the lateral position of the EV is adjusted at each time-step (*i.e.,* every 200ms), which is the default position update frequency. On the other hand, a prediction frequency of $X\%$ ($X < 100$) means that only $X\%$ of the total number of predictions, *i.e.,* 600 predictions, are made.

Fig. 8 depicts the average electromagnetic strength obtained with our solution and the base approach by varying the size of the training dataset. The figure also displays the optimal charging efficiency which is basically the average of the greatest electromagnetic strength measured at each time step. Overall, the result shows substantial improvement of the charging efficiency for our solution. It was observed that our solution enhances the charging efficiency by up to 174% compared to that of the base approach, clearly demonstrating the opportunity to significantly boost the charging efficiency through the lateral position adjustment of the EV in response to the dynamically changing electromagnetic field.

Fig. 9 exhibits the charging efficiency measured by varying the prediction frequency. We observed that the charging efficiency decreased by 57% as the prediction frequency was lowered to 20% from 100%, indicating that to cope better with the dynamically changing electromagnetic field, frequent EV motion control is required. Although a higher prediction frequency results in improved charging efficiency, it should be noted that the higher prediction frequency can affect the level of driver comfort due to frequent EV motion adjustments. Therefore, an experimental study is conducted to analyze the trade-off between driver comfort and charging efficiency, and to determine an appropriate value for the prediction frequency is performed in Section V-C.

C. Driver Comfort

We demonstrated that more frequent predictions led to higher charging efficiency. However, adjusting the EV motion too often can negatively affect the level of driver comfort. In particular, a directly related parameter of our solution that can be used to control the prediction frequency more precisely is f which represents the future time horizon for prediction. The default value for the parameter is 1, which means that a prediction is made at each time-step, *i.e.,* every 200ms.

Noting that the prediction interval of 200m is too small, in this experiment, we set the value of parameter f to 15 to ensure that the driver's comfort level is not impacted. More specifically, the value of 15 for parameter f indicates that a prediction is made every 3 seconds. Considering that the standard lane width of the highway in U.S. is about 3.6m, the minimum lateral acceleration (for a typical passenger car with a width of 2m) to complete adjustment of the EV position within 3 seconds is 0.36m/s^2, which is easily within the 50% comfort threshold for the lateral acceleration of 1.18m/s^2 [40].

Authorized licensed use limited to: WICHITA STATE UNIVERSITY LIBRARIES. Downloaded on September 09,2025 at 19:54:10 UTC from IEEE Xplore. Restrictions apply.

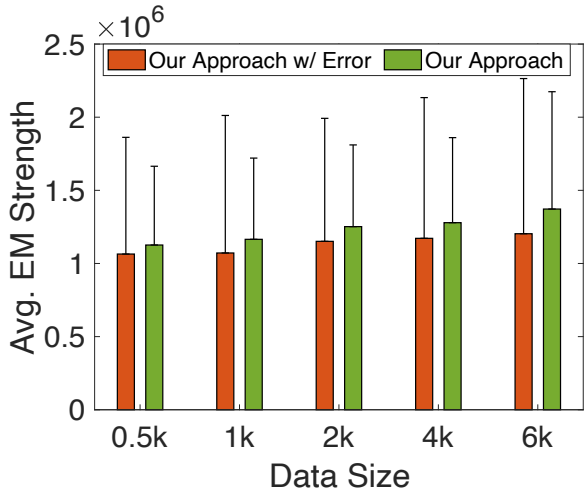

Fig. 11. The effect of the localization error on charging efficiency. A slight decrease in the charging efficiency is observed when the localization error was added to the predicted point.

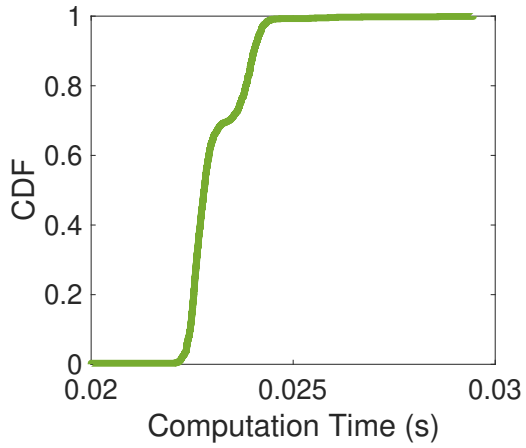

Fig. 12. Cumulative distribution function (CDF) graph for the computational delay. The average computational delay is small enough to support the high prediction frequency.

In other words, we allow for more time for the EV to adjust its lateral position smoothly, thereby minimizing the impact on driver comfort. Fig. 10 depicts the charging efficiency for the two different values for parameter f. We observed that the charging efficiency with $f = 15$ was lower than that for $f = 1$. However, it is worth noting that despite the degraded charging efficiency, our LSTM model with $f = 15$ still performs significantly better than the base approach by 150%, demonstrating that the charging efficiency can be greatly enhanced with only a small impact on driver comfort.

D. Motion Control Accuracy

Another very important factor that can affect the performance is the EV positioning error caused by the imprecision of the EV motion control system. Recent advances in vehicle positioning systems based on fusion of various types of sensors, especially LiDAR sensors, significantly reduced the lateral positioning error down to 7 to 9cm on average [41], [42]. In this section, we analyze the performance of our approach assuming that the localization error occurs with an average of 8cm. More specifically, a random localization error by up to 8cm was added to the predicted point when we measure the charging efficiency. The results are depicted in Fig. 11. We observe that the charging efficiency degraded by about 12% when localization errors were introduced, regardless of the training dataset size.

E. Computational Delay

We have demonstrated in Section V-B that more frequently adjusting the lateral position of the EV led to higher charging efficiency. One important requirement to perform position adjustment frequently is the low computational delay for predicting the optimal lateral position. We measured the computational delay 1,000 times to confirm that the prediction is made fast enough to support the high prediction frequency. Fig. 12 depicts the cumulative distribution function (CDF) graph of the measured computational delay. The results demonstrate that in more than 95% of cases, the computational delay is smaller than 25ms, and the average computational delay is 23.8ms, which is small enough to perform predictions very quickly.

VI. Conclusion

We have presented an LSTM-based adaptive vehicle motion control system for DWC designed to optimize charging efficiency. The dynamics of the electromagnetic field generated from the transmitter coils are effectively captured using a machine learning model. A multi-layer LSTM model is designed to allow an EV to predict the optimal point where the maximum electromagnetic strength is expected and adjust its lateral position before it reaches that point. Extensive simulation results demonstrate that our approach achieves by up to 174% higher charging efficiency compared with a state-of-the-art solution that is designed to position the EV in the center of the lane.

Our research suggests several research directions for future work. One direction is to overcome the limitations of simulation-based evaluations by implementing a prototype DWC system, based on autonomous RC cars, integrated with our proposed LSTM-based EV motion control solution. This would demonstrate enhanced charging efficiency in a more realistic setting for a dynamic wireless charging system. Another area of focus should be addressing scalability limitations by conducting city-scale simulations. This would help in understanding the broad societal and economic impacts of the proposed EV motion control system, potentially leading to significant energy savings. We also intend to examine the possible negative effects of fully automated EV motion control systems on the comfort and safety of human-driven vehicles nearby. Further, developing a more generalizable LSTM model suitable for diverse dynamic EV charging environments remains a crucial future endeavor.

Authorized licensed use limited to: WICHITA STATE UNIVERSITY LIBRARIES. Downloaded on September 09,2025 at 19:54:10 UTC from IEEE Xplore. Restrictions apply.

REFERENCES

[1] D. Patil, M. K. Mcdonough, J. M. Miller, B. Fahimi, and P. T. Balsara, "Wireless power transfer for vehicular applications: Overview and challenges," *IEEE Transactions on Transportation Electrification*, vol. 4, no. 1, pp. 3–37, 2017.

[2] G. Guidi, A. M. Lekkas, J. E. Stranden, and J. A. Suul, "Dynamic wireless charging of autonomous vehicles: Small-scale demonstration of inductive power transfer as an enabling technology for self-sufficient energy supply," *IEEE Electrification Magazine*, vol. 8, no. 1, pp. 37–48, 2020.

[3] N. M. Imran and M. Won, "Reducing operation cost of lpwan roadside sensors using cross technology communication," *IEEE Transactions on Intelligent Transportation Systems*, vol. 23, no. 8, pp. 11 476–11 489, 2021.

[4] N. M. Imran, S. Mishra, and M. Won, "A-vrpd: Automating drone-based last-mile delivery using self-driving cars," *IEEE Transactions on Intelligent Transportation Systems*, 2023.

[5] ——, "Towards fully autonomous drone-based last-mile delivery," *arXiv preprint arXiv:2103.04118*, 2021.

[6] D. Patil, J. M. Miller, B. Fahimi, P. T. Balsara, and V. Galigekere, "A coil detection system for dynamic wireless charging of electric vehicle," *IEEE Transactions on Transportation Electrification*, vol. 5, no. 4, pp. 988–1003, 2019.

[7] A. Ahmad, M. S. Alam, and R. Chabaan, "A comprehensive review of wireless charging technologies for electric vehicles," *IEEE Transactions on Transportation Electrification*, vol. 4, no. 1, pp. 38–63, 2017.

[8] S. Lukic and Z. Pantic, "Cutting the cord: Static and dynamic inductive wireless charging of electric vehicles," *IEEE Electrification Magazine*, vol. 1, no. 1, pp. 57–64, 2013.

[9] J. Bolger, F. Kirsten, and L. Ng, "Inductive power coupling for an electric highway system," in *28th IEEE Vehicular Technology Conference*, vol. 28, 1978, pp. 137–144.

[10] C. C. Mi, G. Buja, S. Y. Choi, and C. T. Rim, "Modern advances in wireless power transfer systems for roadway powered electric vehicles," *IEEE Transactions on Industrial Electronics*, vol. 63, no. 10, pp. 6533–6545, 2016.

[11] S. Moon, B.-C. Kim, S.-Y. Cho, C.-H. Ahn, and G.-W. Moon, "Analysis and design of a wireless power transfer system with an intermediate coil for high efficiency," *IEEE Transactions on Industrial Electronics*, vol. 61, no. 11, pp. 5861–5870, 2014.

[12] F. van der Pijl, P. Bauer, and M. Castilla, "Control method for wireless inductive energy transfer systems with relatively large air gap," *IEEE Transactions on Industrial Electronics*, vol. 60, no. 1, pp. 382–390, 2011.

[13] C. Panchal, S. Stegen, and J. Lu, "Review of static and dynamic wireless electric vehicle charging system," *Engineering Science and Technology, an International Journal*, vol. 21, no. 5, pp. 922–937, 2018.

[14] Z. Chen, W. Jing, X. Huang, L. Tan, C. Chen, and W. Wang, "A promoted design for primary coil in roadway-powered system," *IEEE Transactions on Magnetics*, vol. 51, no. 11, pp. 1–4, 2015.

[15] K. Hwang, J. Cho, D. Kim, J. Park, J. H. Kwon, S. I. Kwak, H. H. Park, and S. Ahn, "An autonomous coil alignment system for the dynamic wireless charging of electric vehicles to minimize lateral misalignment," *Energies*, vol. 10, no. 3, p. 315, 2017.

[16] Y. Tian, Z. Zhu, L. Xiang, and J. Tian, "Vision-based rapid power control for a dynamic wireless power transfer system of electric vehicles," *IEEE Access*, vol. 8, pp. 78 764–78 778, 2020.

[17] W. Chen, C. Liu, C. H. Lee, and Z. Shan, "Cost-effectiveness comparison of coupler designs of wireless power transfer for electric vehicle dynamic charging," *Energies*, vol. 9, no. 11, p. 906, 2016.

[18] J. P. W. Chow, N. Chen, H. S. H. Chung, and L. L. H. Chan, "An investigation into the use of orthogonal winding in loosely coupled link for improving power transfer efficiency under coil misalignment," *IEEE Transactions on Power Electronics*, vol. 30, no. 10, pp. 5632–5649, 2014.

[19] J. Shin, S. Shin, Y. Kim, S. Ahn, S. Lee, G. Jung, S.-J. Jeon, and D.-H. Cho, "Design and implementation of shaped magnetic-resonance-based wireless power transfer system for roadway-powered moving electric vehicles," *IEEE Transactions on Industrial Electronics*, vol. 61, no. 3, pp. 1179–1192, 2013.

[20] J. Kim, J. Kim, S. Kong, H. Kim, I.-S. Suh, N. P. Suh, D.-H. Cho, J. Kim, and S. Ahn, "Coil design and shielding methods for a magnetic resonant wireless power transfer system," *Proceedings of the IEEE*, vol. 101, no. 6, pp. 1332–1342, 2013.

[21] Y.-S. Byun, R.-G. Jeong, and S.-W. Kang, "Vehicle position estimation based on magnetic markers: Enhanced accuracy by compensation of time delays," *Sensors*, vol. 15, no. 11, pp. 28 807–28 825, 2015.

[22] L. C. Das, D. Dasgupta, and M. Won, "Lstm-based adaptive vehicle position control for dynamic wireless charging," *arXiv preprint arXiv:2205.10491*, 2022.

[23] K. A. Kalwar, S. Mekhilef, M. Seyedmahmoudian, and B. Horan, "Coil design for high misalignment tolerant inductive power transfer system for EV charging," *Energies*, vol. 9, no. 11, p. 937, 2016.

[24] Y. Gao, K. B. Farley, and Z. T. H. Tse, "A uniform voltage gain control for alignment robustness in wireless ev charging," *Energies*, vol. 8, no. 8, pp. 8355–8370, 2015.

[25] P. Hu, J. Ren, and W. Li, "Frequency-splitting-free synchronous tuning of close-coupling self-oscillating wireless power transfer," *Energies*, vol. 9, no. 7, p. 491, 2016.

[26] R. Tavakoli, E. M. Dede, C. Chou, and Z. Pantic, "Cost-efficiency optimization of ground assemblies for dynamic wireless charging of electric vehicles," *IEEE Transactions on Transportation Electrification*, 2021.

[27] H.-G. Ryu and D. Har, "Wireless power transfer for high-precision position detection of railroad vehicles," in *2015 IEEE Power, Communication and Information Technology Conference (PCITC)*, 2015, pp. 605–608.

[28] C. Shuwei, L. Chenglin, and W. Lifang, "Research on positioning technique of wireless power transfer system for electric vehicles," in *2014 IEEE Conference and Expo Transportation Electrification Asia-Pacific (ITEC Asia-Pacific)*, 2014, pp. 1–4.

[29] Y. Choi, D. Kang, S. Lee, and Y. Kim, "The autonomous platoon driving system of the on line electric vehicle," in *2009 ICCAS-SICE*, 2009, pp. 3423–3426.

[30] H.-G. Xu, M. Yang, C.-X. Wang, and R.-Q. Yang, "Magnetic sensing system design for intelligent vehicle guidance," *IEEE/ASME Transactions on Mechatronics*, vol. 15, no. 4, pp. 652–656, 2009.

[31] K. Hwang, J. Park, D. Kim, H. H. Park, J. H. Kwon, S. I. Kwak, and S. Ahn, "Autonomous coil alignment system using fuzzy steering control for electric vehicles with dynamic wireless charging," *Mathematical Problems in Engineering*, vol. 2015, 2015.

[32] TeraAnalysis, "QuickField," http://https://quickfield.com/, 2022, accessed: 2022-01-3.

[33] C. Zhang, W. Wang, C. Xu, and J. Yang, "Research on uniform magnetic field compensation structure of array circular coils for wireless power transfer," *IEEE Transactions on Magnetics*, vol. 57, no. 6, pp. 1–5, 2021.

[34] B. D. Truong, E. Andersen, C. Casados, and S. Roundy, "Magneto-electric wireless power transfer for biomedical implants: Effects of non-uniform magnetic field, alignment and orientation," *Sensors and Actuators A: Physical*, vol. 316, p. 112269, 2020.

[35] Z. Zhang and B. Zhang, "Angular-misalignment insensitive omnidirectional wireless power transfer," *IEEE Transactions on Industrial Electronics*, vol. 67, no. 4, pp. 2755–2764, 2019.

[36] J. Schmidhuber and S. Hochreiter, "Long short-term memory," *Neural Computation*, vol. 9, no. 8, pp. 1735–1780, 1997.

[37] L. Hou, J. Zhu, J. Kwok, F. Gao, T. Qin, and T.-y. Liu, "Normalization helps training of quantized lstm," *Advances in Neural Information Processing Systems*, vol. 32, 2019.

[38] Q. Li, F. Wang, J. Wang, and W. Li, "LSTM-based SQL injection detection method for intelligent transportation system," *IEEE Transactions on Vehicular Technology*, vol. 68, no. 5, pp. 4182–4191, 2019.

[39] D. Cao, Y. Wang, J. Duan, C. Zhang, X. Zhu, C. Huang, Y. Tong, B. Xu, J. Bai, J. Tong, *et al.*, "Spectral temporal graph neural network for multivariate time-series forecasting," *Advances in Neural Information Processing Systems*, vol. 33, pp. 17 766–17 778, 2020.

[40] K. N. de Winkel, T. Irmak, R. Happee, and B. Shyrokau, "Standards for passenger comfort in automated vehicles: Acceleration and jerk," *Applied Ergonomics*, vol. 106, p. 103881, 2023.

[41] K. Kim, J. Im, and G. Jee, "Tunnel facility based vehicle localization in highway tunnel using 3d lidar," *IEEE Transactions on Intelligent Transportation Systems*, 2022.

[42] N. Steinke, C.-N. Ritter, D. Goehring, and R. Rojas, "Robust lidar feature localization for autonomous vehicles using geometric fingerprinting on open datasets," *IEEE Robotics and Automation Letters*, vol. 6, no. 2, pp. 2761–2767, 2021.

Authorized licensed use limited to: WICHITA STATE UNIVERSITY LIBRARIES. Downloaded on September 09,2025 at 19:54:10 UTC from IEEE Xplore. Restrictions apply.